NASA CR-121256

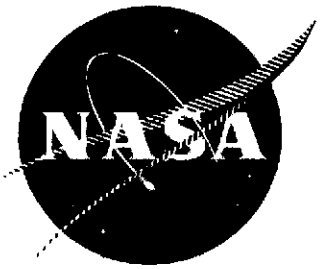

FLOW VISUALIZATION EXPERIMENTS IN A POROUS NOZZLE

by

Z. Cielak, R. B. Kinney, H. C. Perkins

AEROSPACE AND MECHANICAL ENGINEERING DEPARTMENT

UNIVERSITY OF ARIZONA
TUCSON, ARIZONA

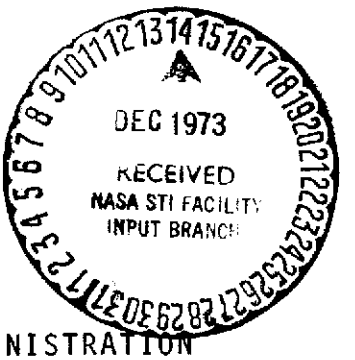

prepared for

NATIONAL AERONAUTICS AND SPACE ADMINISTRATION

NASA Lewis Research Center
Grant NGR 03-002-213

August, 1973

1. Report No.	2. Government Accession No.	3. Recipient's Catalog No.
NASA CR-121256		

4. Title and Subtitle	5. Report Date
FLOW VISUALIZATION EXPERIMENTS IN A POROUS NOZZLE	August 1973
	6. Performing Organization Code

7. Author(s)	8. Performing Organization Report No.
Z. M. Cielak, R. B. Kinney, H. C. Perkins	
	10. Work Unit No.

9. Performing Organization Name and Address	11. Contract or Grant No.
Aerospace and Mechanical Engineering Department University of Arizona Tucson, Arizona 85721	NGR 03-002-213
	13. Type of Report and Period Covered
12. Sponsoring Agency Name and Address	Contractor Report
National Aeronautics and Space Administration Washington, D. C. 20546	14. Sponsoring Agency Code

15. Supplementary Notes

Project Manager, Albert F. Kascak, Nuclear Systems Division, NASA Lewis Research Center, Cleveland, Ohio.

16. Abstract

An experimental approach is described for the study of nozzle flows with large wall-transpiration rates. Emphasizing a qualitative understanding of the flow, the technique uses the hydraulic analogy, whereby a compressible gas flow is simulated by a water flow having a free surface. For simplicity, the simulated gas flow is taken to be two-dimensional. A nozzle with porous walls in the throat region has been developed for use on a water table. A technique for visualizing the transpired fluid has also been devised. These are discussed, and prelimianry results are presented which illustrate the success of the experimental approach.

17. Key Words (Suggested by Author(s))	18. Distribution Statement
Porous Nozzle Wall Transpiration Flow Visualization Hydraulic Analogy	Unclassified - unlimited

19. Security Classif. (of this report)	20. Security Classif. (of this page)	21. No. of Pages	22. Price*
Unclassified	Unclassified	31	$3.00

* For sale by the National Technical Information Service, Springfield, Virginia 22151

NASA CR-121256

FLOW VISUALIZATION EXPERIMENTS IN A POROUS NOZZLE

by

Z. Cielak, R. B. Kinney, H. C. Perkins

AEROSPACE AND MECHANICAL
ENGINEERING DEPARTMENT

UNIVERSITY OF ARIZONA
TUCSON, ARIZONA

prepared for

NATIONAL AERONAUTICS AND SPACE ADMINISTRATION

NASA Lewis Research Center
Grant NGR 03-002-213

August, 1973

FOREWORD

This report is one of a series of four which describes an investigation into the effects of wall transpiration on the flow in a convergent-divergent nozzle. This work was supported by the Nuclear Systems Division, NASA Lewis Research Center, under Grant NGR 03-002-213. The Technical Manager was Mr. Albert F. Kascak.

TABLE OF CONTENTS

SUMMARY.....1

INTRODUCTION.....2

NOZZLE DESIGN.....3

INJECTION SYSTEM.....5

PRELIMINARY RESULTS.....6

CONCLUDING REMARKS.....10

NOMENCLATURE.....11

REFERENCES.....12

FIGURES.....13

APPENDIX A.....22

SUMMARY

An experimental approach is described for the study of nozzle flows with large wall-transpiration rates. Emphasizing a qualitative understanding of the flow, the technique uses the hydraulic analogy, whereby a compressible gas flow is simulated by a water flow having a free surface. For simplicity, the simulated gas flow is taken to be two-dimensional. A nozzle with porous walls in the throat region has been developed for use on a water table. A technique for visualizing the transpired fluid has also been devised. These are discussed, and preliminary results are presented which illustrate the success of the experimental approach.

INTRODUCTION

Advanced space missions involving long travel time require a rocket engine with high specific impulse (a measure of thrust produced per unit mass of propellant). Recent studies have shown that specific impulses on the order of several thousand seconds are possible with engines employing a gas core nuclear reactor (1,2). In this concept, nuclear energy is thermally radiated to a light propellant gas such as hydrogen. The high temperature propellant (12,000°R and greater), then provides thrust by expanding through a nozzle in the conventional manner.

To render the concept feasible, the nozzle must be protected from the high thermal heat flux. One cooling method under consideration involves the transpiration of large amounts of coolant fluid through the nozzle wall in the throat region. At the present time it is expected that the transpired flow could be as large as 20% of the main nozzle flow.

It is not presently known what effects the large transpiration rates could have on the flow dynamics in the transonic region of the nozzle, nor is it known how the thickness of the layer of coolant fluid adjacent to the wall will vary with the amount of transpiration. The layer of coolant fluid, when it is seeded with an opaque material such as submicron tungsten particles, must be sufficiently thick to absorb a large fraction of the thermal radiation from the hot propellant.

In the present report, an experimental approach is described for the study of nozzle flows with large wall-transpiration rates. Emphasizing a qualitative understanding of the flow, the technique uses the hydraulic analogy whereby a compressible gas flow is simulated by a water flow having a free surface. For simplicity, the simulated gas flow is taken to be two-dimensional. A nozzle with porous walls in the throat region has been developed for use on a water table. A technique for visualizing the transpired fluid has also been devised. These are discussed, and preliminary results are presented which illustrate the success of the experimental approach.

NOZZLE DESIGN

The nozzle test section was modeled after an axi-symmetric nozzle with full size dimensions as shown in Figure 1. This nozzle is identified by the name PIWI and was proposed for use with the solid core nuclear rocket. Since the experiments are to be done in a two-dimensional nozzle, a plane section was taken and appropriately scaled to be compatible with the capacity of the flow circuit. This is explained below.

The porous nozzle is to be mounted in the 4' x 8' test section of the water table described in Reference (3). The test section flow is limited to 80 gallons/minute. For supercritical flow through the nozzle, one-dimensional flow theory shows that the flow rate is a function only of the throat width and upstream stagnation height. This is in analogy with one-dimensional gas dynamics for which the flow rate depends only on the throat area plus the stagnation temperature and pressure.

The maximum upstream stagnation height was selected to be 4.5 inches (the water height at the throat for a critical flow nozzle is two-thirds of this or 3.0 inches). For a throat width of 2.96 inches (which is one-half the dimension of the PIWI nozzle), the maximum flow was calculated to be approximately 78 g.p.m. Since this was below the flow limit, the remaining dimensions of the nozzle were similarly cut in half, thus preserving the nozzle proportions. With the dimensions of the nozzle now specified, a height profile and Froude number distribution were calculated along the nozzle axis using one-dimensional theory. The pertinent relationships are derived in Appendix A. Alternatively, these can be obtained from one-dimensional gas-dynamic relationships by setting the specific-heat ratio equal to 2. The Froude number corresponds to the Mach number, and the ratio of the local and stagnation heights corresponds to the static temperature ratio. These results are shown in Figure 2.

To assure successful nozzle performance and versatility, several conditions had to be met. These are:

(a) Achieving uniform acceleration of the flow while at the same time maintaining it free of disturbance, especially in the throat region where the greatest flow shear is present.

(b) Limiting the injection to the wetted area of the nozzle. This is particularly important since the water height changes continuously in the flow direction and also depends on the initial inlet height. See Figure 2.

(c) Insuring uniform wall injection over the wetted surface of the nozzle.

(d) Having the ability to inject at distinct areas of the nozzle in varying amounts, as well as a means for changing the throat width.

The nozzle design finally selected is illustrated in Figure 3. The nozzle test section consists of three separate sections joined together by a connecting bar. The injection is limited to the middle (injection) section which includes the near-throat region of the nozzle. The wall* of this section is continuous and made of 1/16 inch thick stainless steel multilayer filter type material. (This filter type material will pass particles of forty microns or less.) A separately regulated supply of fluid is connected to each of three compartments in the injection section. These are separated by plates joined to the porous wall by a fine, watertight, and continuous weld.

In order to match the areas wetted by the main nozzle flow, the height of the plenums behind the porous sections had to be adjustable. This was accomplished by flexible diaphragms made of highly tear-resistant, room temperature vulcanizing (RTV) rubber which are guided and driven by closely spaced threaded rods. This permits the diaphragm setting to conform to the water level, blocking possible injection above the main flow.

To minimize the deterioration of the nozzle operating in a somewhat corrosive environment, stainless-steel, aluminum, and plexiglass were chosen as the predominant construction materials. The upstream and downstream sections are made of formed plexiglass walls. Changing the shape of these sections, which can be fabricated with minimum expense and difficulty, permits the basic nozzle shape to be changed. Also, since the nozzle walls are separate and symmetrical units, they may be set to any desired width as well as rotated to different angles of expansion.

---

*The nozzle being symmetrical, reference will be made to only one "wall" since the opposite wall is a mirror image of the one discussed.

To simplify the positioning of the half-size PIWI nozzle, a template machined to the inside dimensions of the nozzle was used. This also allowed contour specifications to be easily read from the template. Figures 4 and 5 show the nozzle positioned on the water table. The honeycomb pieces visible in the upstream region are used to straighten the flow approaching the nozzle. The plastic tubes connecting the inlets of the separated segments of the injection section are independently supplied and controlled. Also, in order to assure stable fluid injection, a special injection system was devised. This is considered next.

INJECTION SYSTEM

The main components of the injection system are shown schematically in Figure 6. These consist of a constant volume pump, surge tank, injection tank, and flow meters. The water table components are described in (3).

Water pumped from the overflow tank 1, by the constant volume pump 4, is filtered before entering the pressurized surge tank 6. The excess water is returned to the overflow tank, the amount of return flow being controlled by valve 15. The flow from the surge tank is filtered again before entering the manifold 9. Upstream of the manifold, additional fluid may be added for purposes of flow visualization. From the manifold, the flow rates through the six lines are measured with rotameters 10. Downstream of the meters, flow control valves 11 are used to regulate the desired amount of flow supplied to the individual porous nozzle sections.

In order to distinguish the flow injected through the porous nozzle walls from the main flow, a system for fluid coloring was devised. This makes use of the color change with hydrogen ion concentration (pH) in aqueous solutions of acids and bases.

To prepare for flow visualization, acetic acid, $HC_2H_3O_2$, is added to the main fluid system and mixed thoroughly. The procedure is to add acetic acid in 100 ml. quantities with a pH measurement after each addition until the pH is in the range from 5.0 to 5.5. Bromothymol-blue pH indicator is then added to the acid solution, coloring it a pale yellow.

The injected fluid is colored blue by continuously adding concentrated sodium hydroxide (pH > 11) at the mixing section 8. This strong base mixes with the weak acid leaving

tank 6, yielding a pH of 8.5-9.0 and a blue tint to the fluid supplied to the nozzle sections. The contrast between the blue and yellow streams can be maintained for more than a minute of continuous running. This is sufficient for most photographic records to be taken. To increase the running time, the fluid in the overflow tank can be neutralized or made basic.

After continued operation of the water table with flow visualization, the main stream fluid will turn green and then blue due to the mixing with the injected fluid. Acid is then added to the main flow in order to return the pH to approximately 5.5. It should be noted that the pH indicator need not be added again in the same quantities prior to successive start-up of the system provided the water solutions are not discharged. After each shut-down, the two fluid systems are neutralized.

PRELIMINARY RESULTS

Tests have been performed in order to substantiate the experimental approach adopted for this study. These have been directed toward (1) a verification that the compressible gas flow is indeed modeled by the water flow through the hydraulic analogy, and (2) a demonstration of the versatility of the flow visualization technique.

Verification of the Hydraulic Analogy

The hydraulic analogy is known to be applicable when the depth changes in a direction perpendicular to the water table surface are relatively small. This usually requires stagnation water depths on the order of one inch or less. However, it is not possible to operate the porous nozzle with wall transpiration when the stagnation water depth is less than approximately 2.5 inches. At lower depths than this, the wetted surface area of the nozzle is too small to allow accurate control of the transpired flow downstream of the throat (see Figure 5). Therefore, in order to verify that water-table flows still simulate compressible gas flows even for these moderately large water depths, comparisons between measured water table data and those for air flow reported in (4) were made.

The experiments reported in (4) were performed using an axi-symmetric nozzle with a convergence angle (measured from the axis) of 45° upstream of the throat and a divergence angle of 15° downstream. These angles correspond exactly to those adopted for the porous nozzle described in the present report. Because the experiments in (4) were performed without wall transpiration, the data comparison will be made only for the case of no injection.

The Froude number, F, measured on the water table is analogous to the Mach number, M, in the compressible air flow. However, one-dimensional flow theory shows that the F and M are equal only when the specific heat ratio for the gas flow is equal to 2. Therefore, a correction for specific heat ratio had to be applied before a direct comparison for these two quantities could be made. The procedure for making this correction is described below.

The correction factor for specific heat ratio has been presented by Adams (5) and is based on the fact that the area-ratio for the compressible gas flow should correspond directly to the width-ratio for the water-table flow. These ratios can be written

$$\frac{A}{A_{th}} = \frac{1}{M}\left[\left(\frac{2}{\gamma+1}\right)\left(1 + \frac{\gamma-1}{2} M^2\right)\right]^{(\gamma+1)/2(\gamma-1)} \qquad (1)$$

$$\frac{B}{B_{th}} = \frac{1}{F}\left[\frac{2}{3}\left(1 + \frac{F^2}{2}\right)\right]^{3/2} \qquad (2)$$

The latter result is derived in Appendix A. If one equates these two expressions, a single equation for M results which can be solved using specified values of γ and F. The thus obtained value of M will be called the "corrected Froude number."

Because of the implicit nature of the equation for M, obtained from equating Equations (1) and (2), it is expedient to use a set of tables giving A/A_{th} and B/B_{th} in terms of M and F, respectively. One first obtains the water-table Froude number from experimental measurements of the local-to-stagnation height ratio, H/H_o. This relationship is derived in Appendix A and is given by,

$$F = [\ 2\ (\frac{H_o}{H} - 1)]^{1/2} \qquad (3)$$

The values of H/H_o and F are then tabulated for each value of B/B_{th} corresponding to the actual geometry of the water-table nozzle. Since the real flow is not one-dimensional there is a distribution of F transverse to the flow direction at a given value of B/B_{th}. These local values of F are then used to calculate an "equivalent" local B/B_{th} from Equation (2). Equating this equivalent B/B_{th} to A/A_{th} for the gas nozzle, the value of M is read from one-dimensional gas-flow tables for $\gamma = 1.4$. This value of M is the corrected Froude number corresponding to the actual value of B/B_{th} for the nozzle, not the equivalent B/B_{th} as calculated from Equation (2).

In the above manner, the corrected Froude number was obtained at locations along the axis of the nozzle. These are shown plotted as the open circles in Figure 7. The solid circles are the Mach numbers obtained from the air-flow experiments of (4). It can be seen that the results are essentially indistinguishable from one another.

Of particular interest is the fact that the corrected Froude and Mach numbers are less than unity at the physical throats of the two nozzles (B/B_{th} and A/A_{th} equal to 1). This is contrary to the predictions of one-dimensional flow theory and is caused by the actual two-dimensional character of the flow.

The two-dimensionality of the water-table flow is further illustrated in Figure 8. Here contours of constant corrected Froude number are shown. These have been obtained in the manner described above. The curves have the same characteristic shape displayed by the Mach number contours found in (4). These results give further support to the modeling capability of the water-table flows. A more extensive presentation of water-table data, including results which show effects of wall transpiration, is contained in (6).

Flow Visualization

Photographs of the flow patterns obtained from the water table tests are shown in Figures 9 and 10. The former corresponds to the case of no wall transpiration, in which it can be seen that the variation in water height (in a direction perpendicular to the plane) produces a pronounced

distortion of the straight lines ruled at one-inch intervals along the table surface. Figure 10 shows the effect of wall transpiration on the main flow. The transpired fluid is colored blue using the acid-base indicator method described earlier.

The mass flow injected through the porous wall is approximately equal for the two porous sections upstream of and including the physical throat. The mass injection downstream of the throat is approximately one-half the upstream values. If subscripts 1, 2, and 3 denote the sections ordered from the upstream to downstream ends, the injected mass flows, expressed as a percentage of the main flow entering the nozzle, are given as follows: $\dot{m}_1 = 3.3\%$, $\dot{m}_2 = 3.3\%$, $\dot{m}_3 = 1.65\%$. These values correspond to injection on one half of the nozzle. The total percentage of injected fluid is obtained by adding these three quantities and multiplying by two. It is seen that this corresponds to an injection rate equal to 16.5% of the flow entering the nozzle.

Some experiments have also been made in order to obtain a qualitative comparison of porous-nozzle flows on the water table and in an actual gas flow. A two-dimensional nozzle with porous walls was constructed with convergence-divergence angles equal to those used on the water table. Using air injected into air, Schlieren photographs were taken with the porous walls of the nozzle forming the throat in a supersonic wind tunnel.

Wall transpiration was regulated through three different sections in each of the nozzle walls just as in the case of the water-table experiments. Mass flow percentages were set equal to those reported earlier in connection with Figure 10. No special technique was used to visualize the injected gas layer next to the wall.

Figure 11 shows a composite Schlieren photograph taken of the air flow. The upper half corresponds to no wall injection, whereas the lower photograph shows the effect of wall transpiration. Downstream of the throat, the wall layer on the lower half of the nozzle appears dark due to the higher density of the injected air. Upstream of the throat the density difference is too small to be visualized. It can be seen that the apparent thickness of the transpired fluid layer is comparable to that visualized on the water table. Also, the oblique wave patterns in the divergent portion of the nozzles are qualitatively the same.

CONCLUDING REMARKS

The basic features of a porous-nozzle test section for use on the water table have been described. Preliminary experiments using the test section have demonstrated that the important phenomena connected with a compressible gas-flow through an impermeable converging-diverging nozzle can be simulated by the water table flow through the hydraulic analogy. From local water-depth measurements, the distribution of the analogous Mach number within the flow can be obtained. These have been shown to be qualitatively the same as those measured in compressible air-flow experiments using an axisymmetric nozzle.

A technique for visualizing the water-table flow through a porous nozzle with wall transpiration has also been described. By coloring the transpired fluid differently from the main nozzle flow, the wall layer affected by the transpiration can be visualized. Photographic records clearly show the extent of the wall layer. This can be related to the transpiration rate at the wall.

A detailed study of the water-table flow through a nozzle with wall transpiration is presented in a companion report, Reference (6). A more extensive development of the flow equations, including the effects of wall transpiration, is presented for the water and compressible gas flows.

NOMENCLATURE

A = flow area

B = width of water flow

c = integration constant

F = Froude number, $V/\sqrt{gH}$

g = local acceleration of gravity

H = water height

M = Mach number

$\dot{m}$ = mass flow percentage

P = static pressure

V = flow velocity

γ = ratio of specific heats of gas

ρ = density

Subscripts

o = stagnation conditions

th = nozzle throat

REFERENCES

(1) Taylor, M. F.; Whitmarsh, C. L.; Sirocky, P. J; and Iwanczyk, L. C, The Open-Cycle Gas-Core Nuclear Rocket Engine - Some Engineering Considerations, NASA TM X-67932. Presented at AIAA Second Symposium on Uranium Plasmas, Atlanta, Georgia, November, 1971.

(2) Duke, E. E.; and Houghton, W. J., Gas-Core Nuclear Rocket Engine, J. Spacecraft, 4, p. 1592-1597, 1967.

(3) Fike, R. L.; Kinney, R. B.; and Perkins, H. C., The Design of a Research Water Table, NASA CR-121255, August, 1973.

(4) Cuffel, R. F.; Back, L. H.; and Massier, P. F., Transonic Flowfield in a Supersonic Nozzle with Small Throat Radius of Curvature, AIAA J., 7, p. 1364-1366, 1969.

(5) Adams, D. M., Application of the Hydraulic Analogy to Axisymmetric Nonideal Compressible Gas Systems, J. Spacecraft, 4, p. 359-363, 1967.

(6) Kinney, R. B.; Cielak, Z.; and Perkins, H. C, Flow in a Porous Nozzle with Massive Wall Injection, NASA CR- 134504, August, 1973.

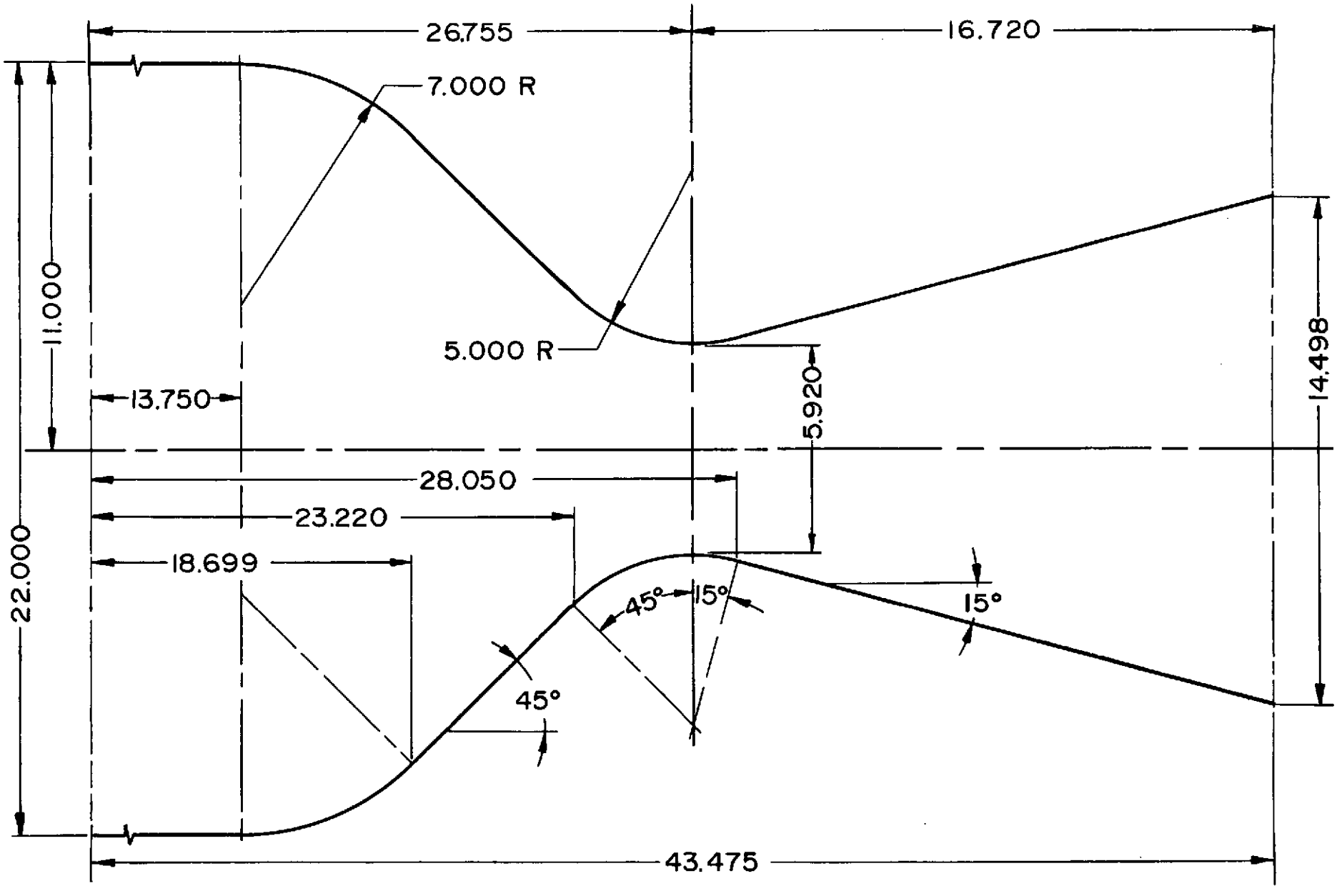

FIGURE 1. FULL-SCALE DIMENSIONS OF THE PIWI AXISYMMETRIC NOZZLE.

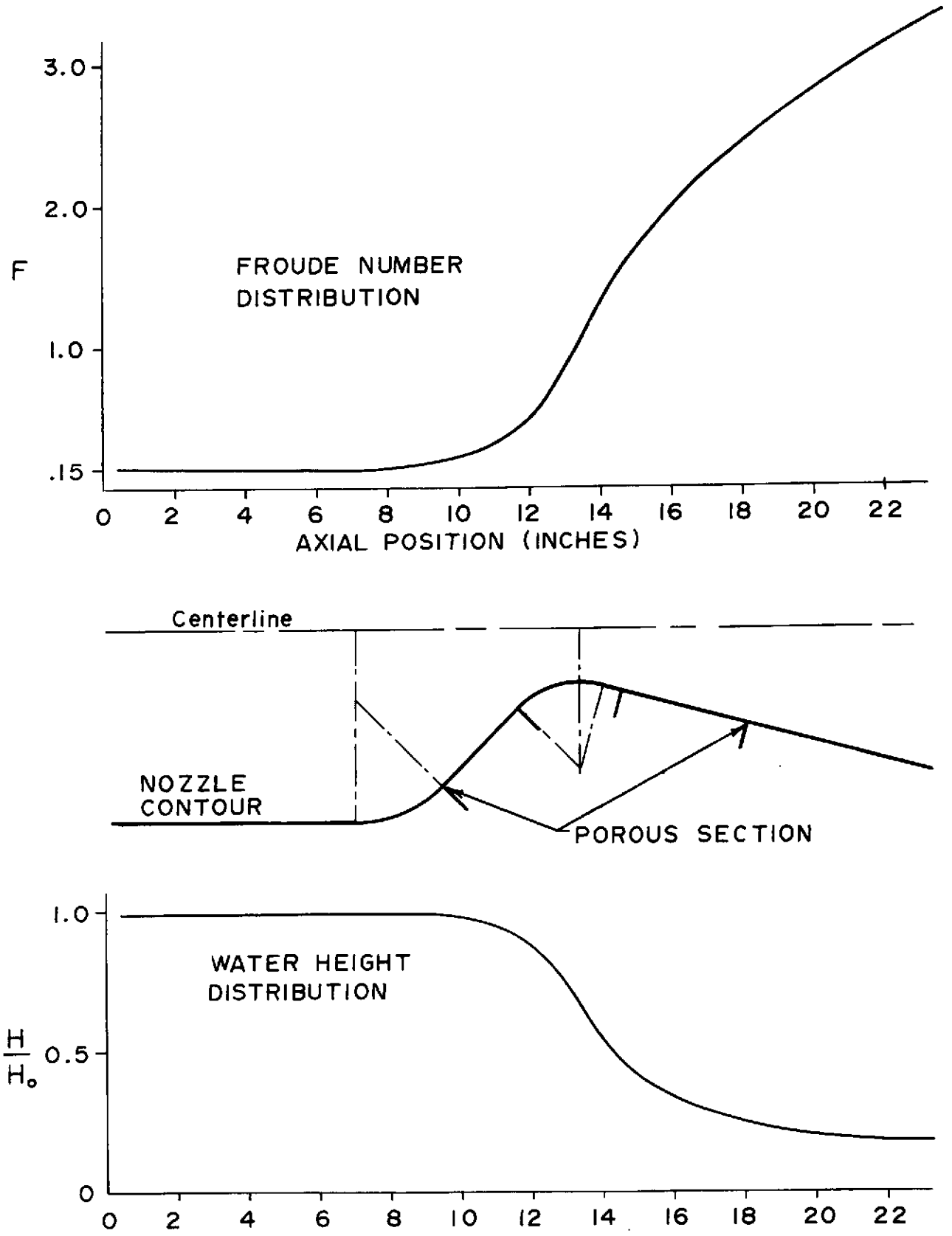

FIGURE 2. FROUDE NUMBER AND WATER-HEIGHT DISTRIBUTIONS PREDICTED BY ONE-DIMENSIONAL FLOW THEORY FOR WATER TABLE NOZZLE.

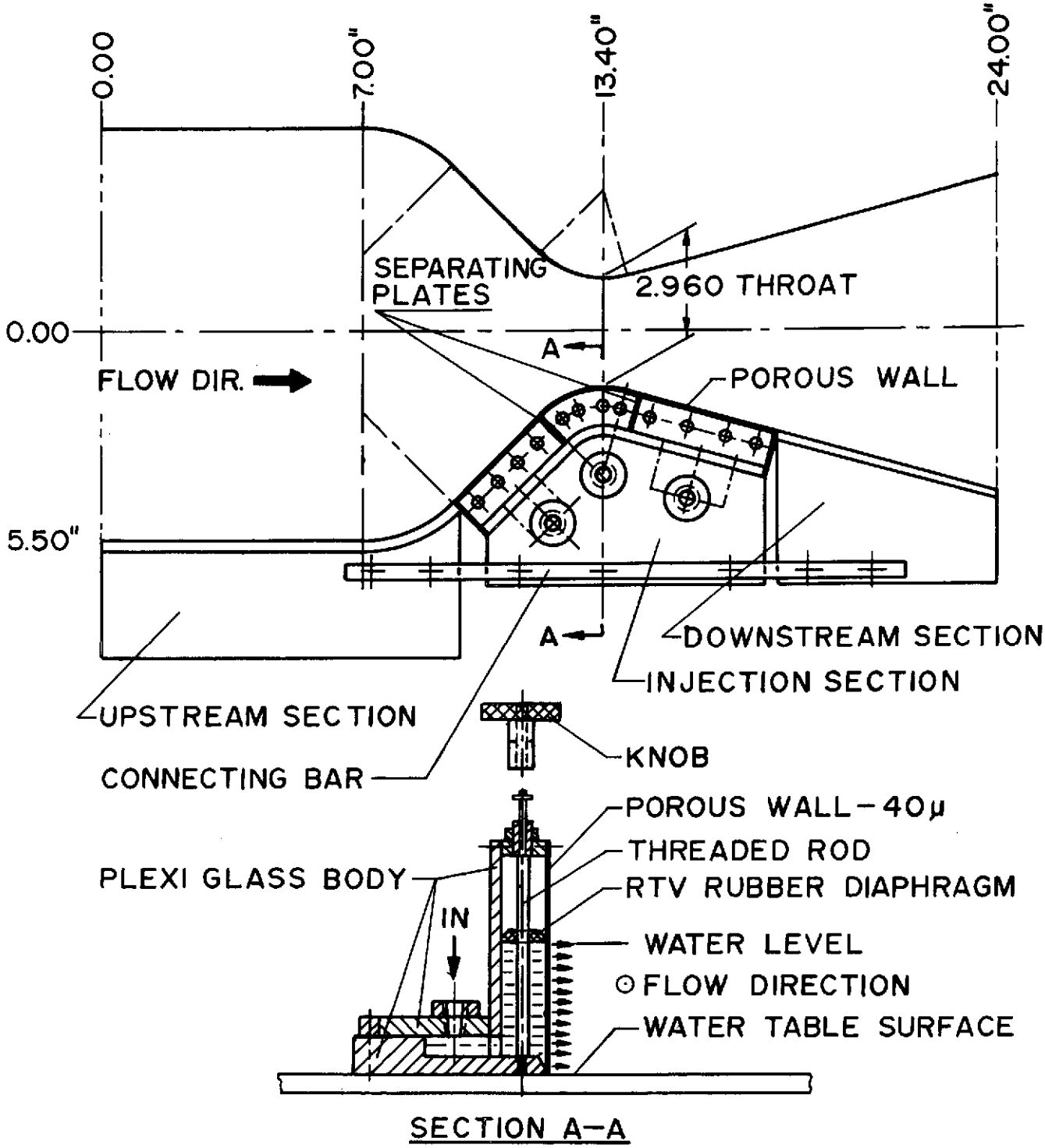

FIGURE 3. DETAIL OF POROUS NOZZLE TEST SECTION.

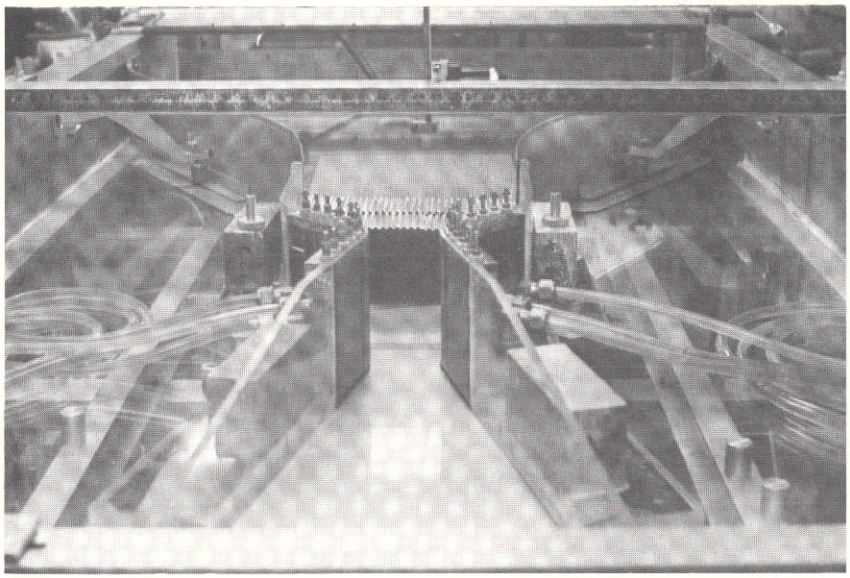

FIGURE 4. POROUS NOZZLE TEST SECTION MOUNTED ON THE WATER TABLE.

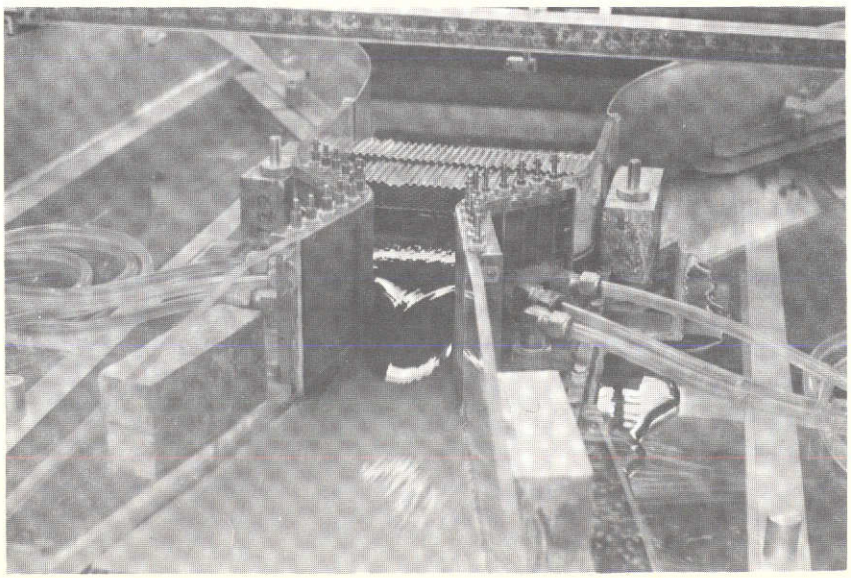

FIGURE 5. WATER FLOW THROUGH POROUS NOZZLE WITHOUT WALL TRANSPIRATION. NOTE SHARP DECREASE IN WATER DEPTH PAST NOZZLE THROAT.

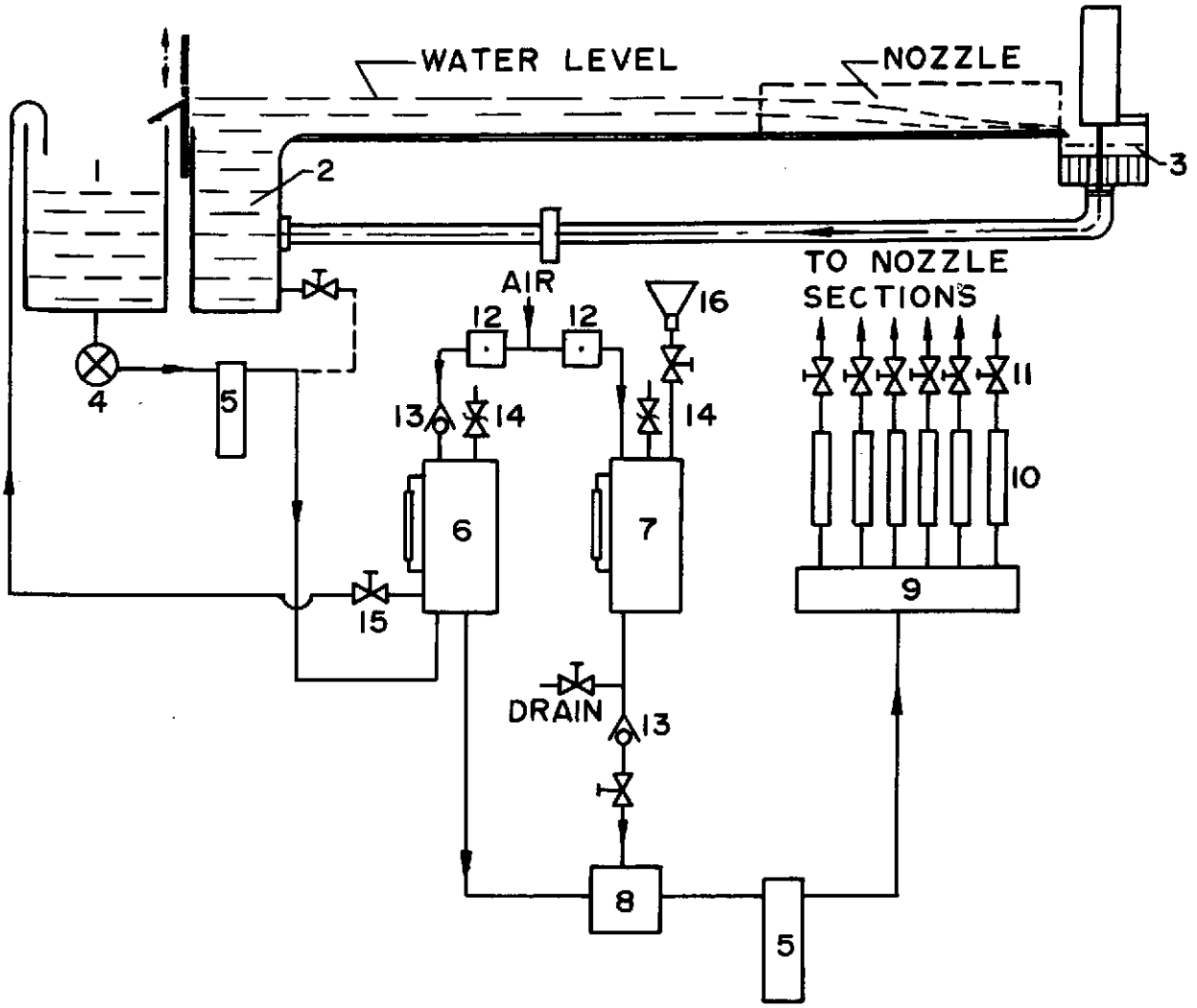

1. OVERFLOW TANK
2. STAGNATION TANK
3. END TANK
4. CONSTANT VOLUME PUMP
5. FILTER
6. SURGE TANK
7. COLORED FLUID TANK
8. MIXER
9. MANIFOLD
10. FLOW METER
11. FLOW CONTROL VALVE
12. AIR REGULATOR
13. CHECK VALVE
14. PRESS. RELIEVE VALVE
15. OVERFLOW CONTROL VALVE
16. FUNNEL

FIGURE 6. SCHEMATIC DIAGRAM OF WATER TABLE AND INJECTION SYSTEM.

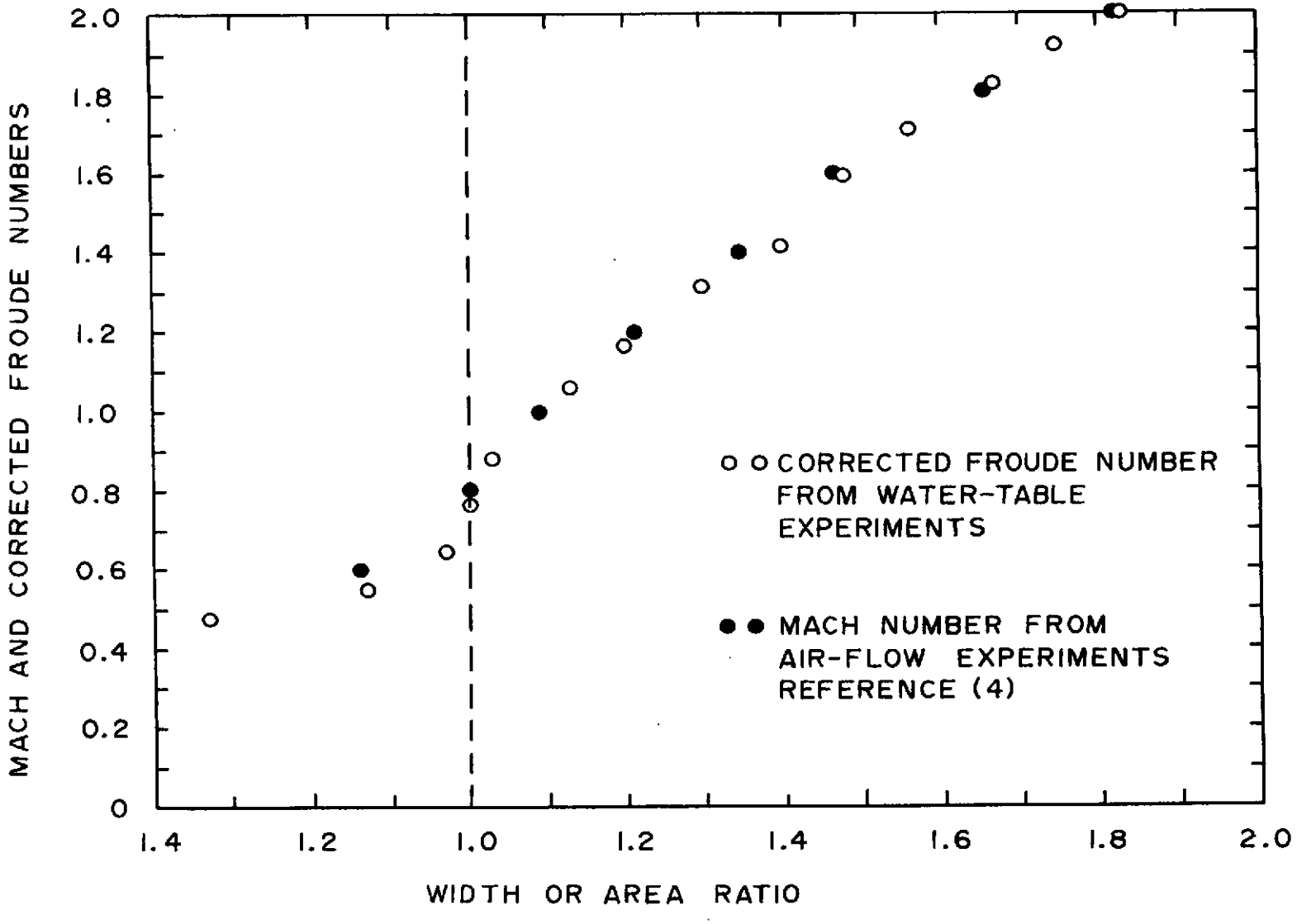

FIGURE 7. COMPARISON OF EXPERIMENTAL MACH AND CORRECTED FROUDE NUMBERS ALONG NOZZLE CENTERLINES, H_0 = 2.83 IN.

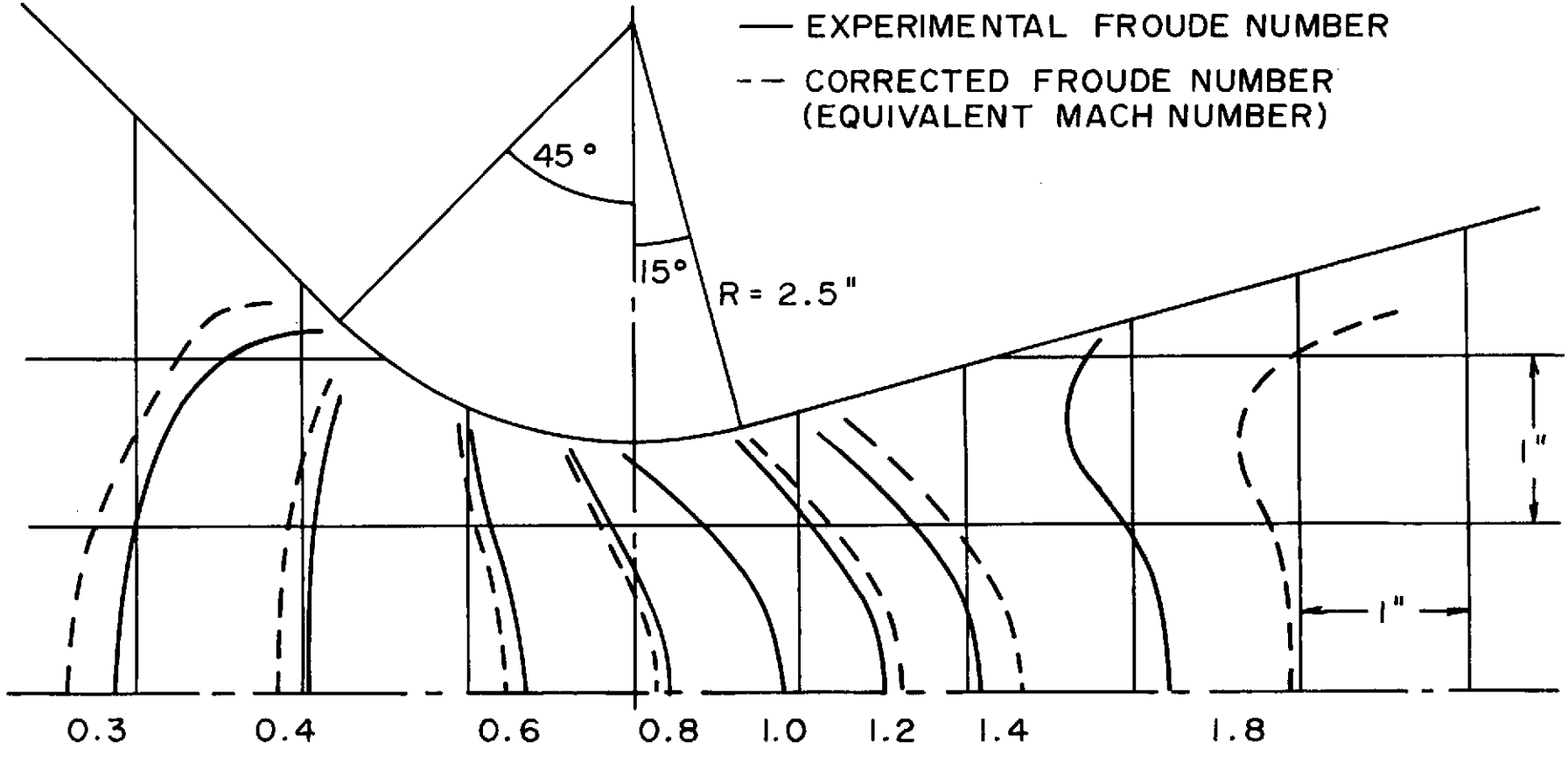

FIGURE 8. CONTOURS OF CONSTANT FROUDE NUMBER THROUGHOUT THE NOZZLE.
H_o = 2.83 IN.

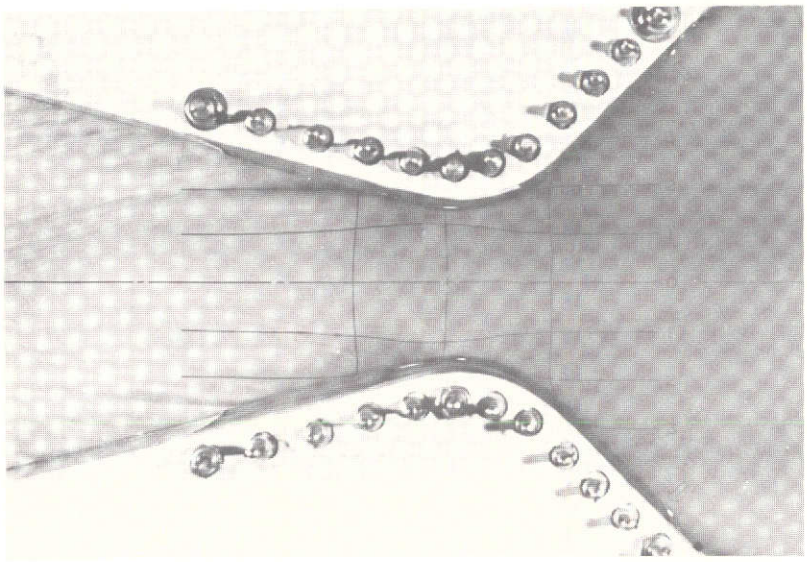

FIGURE 9. NOZZLE FLOW ON WATER TABLE WITHOUT WALL TRANSPIRATION.

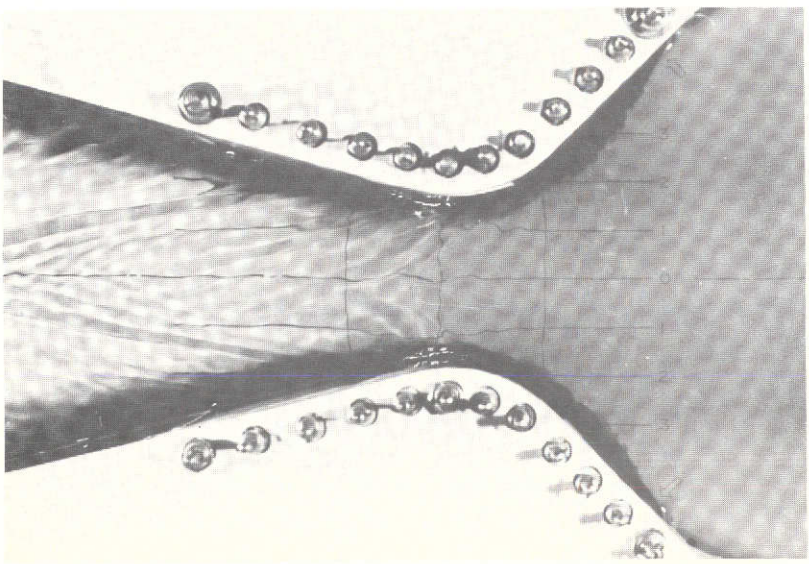

FIGURE 10. NOZZLE FLOW ON WATER TABLE WITH WALL TRANSPIRATION.

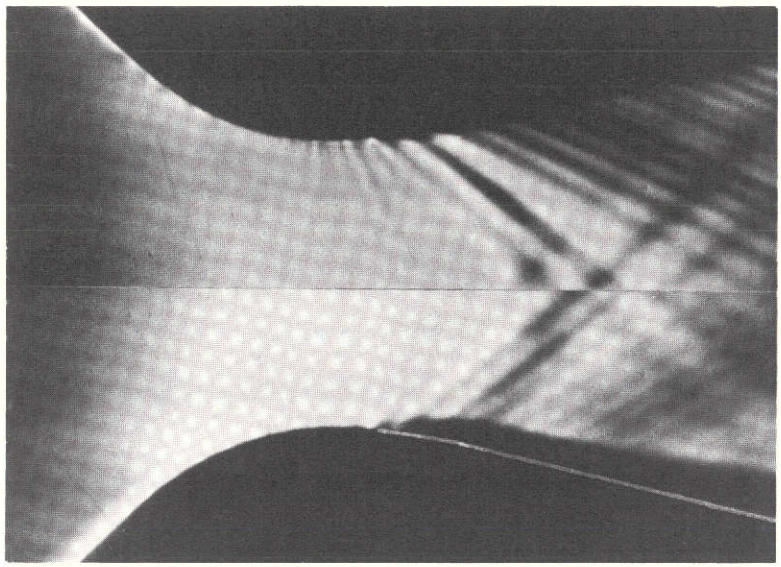

FIGURE 11. COMPOSITE PHOTOGRAPH OF NOZZLE FLOW IN WIND TUNNEL
UPPER HALF - WITHOUT WALL TRANSPIRATION
LOWER HALF - WITH WALL TRANSPIRATION
(WALL DENOTED BY LIGHT LINE)

APPENDIX A

Derivation of Flow Formulas for the Water Table

The basic relationships describing the water flow through a converging-diverging nozzle stem from the equation of continuity and the momentum equation. For a one-dimensional flow (that is, the dependent quantities are functions of only the flow direction, x), these equations are, respectively,

$$V \cdot B \cdot H = \text{constant} \tag{A1}$$

$$V \frac{dV}{dx} = - \frac{1}{\rho} \frac{dP}{dx} \tag{A2}$$

In the foregoing, the fluid is assumed to be frictionless and the nozzle wall is taken to be impermeable. A more general derivation which takes into account fluid transpiration through the nozzle wall is given in (6). The symbols are as defined in the Nomenclature.

A more convenient form of Equation (A2) is obtained if the pressure, P, is taken to be the hydrostatic pressure. That is

$$P = P_{atmospheric} + \rho g H \tag{A3}$$

From this, one obtains

$$\frac{dP}{dx} = \rho g \frac{dH}{dx} \tag{A4}$$

which, when introduced into Equation (A2) yields the following

$$V \frac{dV}{dx} + g \frac{dH}{dx} = 0 \tag{A5}$$

Equations (A1) and (A5) are sufficient to determine V and H for a given nozzle shape (i.e. known variation of B with x).

Relationship Between F and H

The Froude number, F, is related to the flow velocity and water depth through the following definition

$$F = \frac{V}{\sqrt{gH}} \tag{A6}$$

The velocity V can be expressed in terms of H following an integration of Equation (A5) from the stagnation conditions ($H = H_o$ and $V = 0$) to any other point in the flow. Thus

$$H + \frac{V^2}{2g} = H_o \tag{A7}$$

The foregoing is equivalent to the energy equation for the flow. Solving for V, one obtains

$$V = [\, 2g\, (H_o - H)]^{1/2} \tag{A8}$$

After substituting Equation (A8) into Equation (A6) and simplifying, there results

$$F = [\, 2\, (\frac{H_o}{H} - 1)]^{1/2} \tag{A9}$$

This corresponds to Equation (3) given earlier.

Expression for B/B_{th}

Equation (A5) can be written in the equivalent form

$$V\, dV + g\, dH = 0 \tag{A10}$$

Dividing the foregoing by V^2 and substituting $V^2 = gH\,F^2$ into the second term, one obtains

$$\frac{dV}{V} + \frac{1}{F^2}\frac{dH}{H} = 0 \qquad \text{(A11)}$$

The height, H, is given by

$$H = \frac{V^2}{gF^2} \qquad \text{(A12)}$$

from which

$$\ln H = -\ln g + 2\ln V - 2\ln F \qquad \text{(A13)}$$

Upon differentiation, there results

$$\frac{dH}{H} = 2\frac{dV}{V} - 2\frac{dF}{F} \qquad \text{(A14)}$$

One can now eliminate dH/H from Equations (A11) and (A14). Thus

$$(2 + F^2)\frac{dV}{V} = 2\frac{dF}{F} \qquad \text{(A15)}$$

The variables can now be separated and written as exact differentials in the following manner

$$d[\ln V] = d\left[\ln\left(\frac{F^2}{F^2+2}\right)^{1/2}\right] \qquad \text{(A16)}$$

Following a single integration, one obtains

$$V = c\left[\frac{F^2}{F^2+2}\right]^{1/2} \qquad \text{(A17)}$$

where c is the constant of integration.

Let V_{th} denote the critical velocity corresponding to F = 1. Then one has $c = (3)^{1/2} V_{th}$, and finally

$$\frac{V}{V_{th}} = \left[\frac{3F^2}{F^2+2}\right]^{1/2} \tag{A18}$$

The above is a useful expression for the velocity ratio in terms of F.

Continuing, we have from the continuity equation

$$V \cdot B \cdot H = V_{th} \cdot B_{th} \cdot H_{th} \tag{A19}$$

which can be rearranged to give

$$\frac{B}{B_{th}} = \frac{V}{V}th \cdot \frac{H}{H}th \tag{A20}$$

Now, V/V_{th} is given by Equation (A18), and it remains to find H/H_{th}. Recall from Equation (A6) that

$$V^2 = gH\,F^2 \tag{A21}$$

and thus

$$V_{th}^2 = gH_{th} \tag{A22}$$

which gives

$$\frac{H}{H_{th}} = \frac{1}{F^2} \left(\frac{V}{V_{th}}\right)^2 \tag{A23}$$

Substituting Equations (A18) and (A23) into Equation (A20) and rearranging, one obtains the final result

$$\frac{B}{B_{th}} = \frac{1}{F}\left[\frac{2}{3}\left(1 + \frac{F^2}{2}\right)\right]^{3/2} \qquad \text{(A24)}$$

This corresponds to Equation (2) given earlier.

In order to relate B/B_{th} to H/H_o, one notes that from Equation (A7)

$$1 + \frac{F^2}{2} = \frac{H_o}{H} \qquad \text{(A25)}$$

Substituting the above plus Equation (A9) into Equation (A24) and simplifying, one obtains

$$\frac{B}{B_{th}} = \frac{2}{3\sqrt{3}}\left[\left(\frac{H}{H_o}\right)^2 - \left(\frac{H}{H_o}\right)^3\right]^{-1/2} \qquad \text{(A26)}$$